

## Fragmentation of Heavy Quarks Produced in $e^+e^-$ Annihilation

E. Fernandez, W. T. Ford, A. L. Read, Jr., and J. G. Smith

*Department of Physics, University of Colorado, Boulder, Colorado 80309*

and

A. Marini, I. Peruzzi, M. Piccolo, and F. Ronga

*Laboratori Nazionali Frascati dell'Istituto Nazionale di Fisica Nucleare, I-00044 Frascati, Italy*

and

H. T. Blume, J. P. Venuti, and R. Weinstein

*Department of Physics, University of Houston, Houston, Texas 77004*

and

L. A. Baksay, H. R. Band, M. W. Gettner, G. P. Goderre, B. Gottschalk,<sup>(a)</sup> R. B. Hurst,  
O. A. Meyer, J. H. Moromisato, W. D. Shambroom, and E. von Goeler

*Department of Physics, Northeastern University, Boston, Massachusetts 02115*

and

J. V. Allaby,<sup>(b)</sup> W. W. Ash, G. B. Chadwick, S. H. Clearwater, R. W. Coombes,  
Y. Goldschmidt-Clermont,<sup>(b)</sup> H. S. Kaye, K. H. Lau, R. E. Leedy, H. L. Lynch,  
R. L. Messner, S. J. Michalowski,<sup>(c)</sup> K. Rich, D. M. Ritson, L. J. Rosenberg,  
D. E. Wisner, and R. W. Zdarko

*Department of Physics and Stanford Linear Accelerator Center, Stanford University, Stanford, California 94305*

and

D. E. Groom, H. Y. Lee, and E. C. Loh

*Department of Physics, University of Utah, Salt Lake City, Utah 84112*

and

M. C. Delfino, B. K. Heltsley, J. R. Johnson, T. L. Lavine, T. Maruyama, and R. Prepost

*Department of Physics, University of Wisconsin, Madison, Wisconsin 53706*

(Received 19 April 1983)

Identification of muons in hadronic events from  $e^+e^-$  annihilation observed in the MAC detector at the storage ring PEP provides flavor tagging of heavy primary quarks. A sample enriched in events from  $b\bar{b}$  production is obtained and the  $b$ -quark fragmentation function is inferred from the momentum spectrum of the muons. The  $b$  quark is found to fragment predominantly with high values of  $z$ , with  $\langle z_b \rangle = 0.8 \pm 0.1$ , and to have an overall semimuonic branching fraction of  $(15.5^{+2.4}_{-2.9})\%$ .

PACS numbers: 14.80.Dg, 13.20.Jf, 13.65+i

Detection of muons in hadronic events produced in electron-positron annihilation is a signature of weak decays of heavy quarks, and provides a means of tagging events originating from heavy quarks. The spectrum of the muon momentum transverse to the jet direction is determined by the mass of the decaying particle, and can be used to separate events with  $b$  parent quarks from those originating from  $c$  quarks. With this method, fragmentation of the  $b$  quark can be studied by analyzing the momentum spectrum of the muons from  $b$  decay. Several experiments have

reported on the relatively hard fragmentation function of the  $c$  quark,<sup>1</sup> and the only previous published result on  $b$  fragmentation<sup>2</sup> suggests a hard, sharply peaked distribution. On the basis of the inclusive muon spectrum measured by the MAC detector at the electron-positron storage ring PEP at the Stanford Linear Accelerator Center, with center-of-mass energies at or near 29 GeV, we obtain a new, high-statistics determination of the  $b$  fragmentation function.

The MAC detector has been described in detail elsewhere.<sup>3</sup> Briefly, the detector is centered

around a cylindrical drift chamber for tracking charged particles.<sup>4</sup> The chamber consists of ten layers of drift cells, of which six are skewed by  $\pm 3^\circ$  from the beam axis to provide position measurement in all three dimensions. The drift chamber is surrounded by a solenoid coil providing a magnetic field of 5.7 kG, and, in a hexagonal geometry, by a shower chamber followed by a hadron calorimeter. Layers of lead interspersed with proportional wire chambers constitute the shower chamber, amounting to 16 radiation lengths of material. The hadron calorimeter alternates layers of steel with proportional wire chambers, with normally incident particles traversing 90 cm of steel. The hadron calorimeter and the shower chamber are each segmented into 192 azimuthal sectors and three radial layers from which independent readouts are obtained. Charge division is used to determine the axial position of showers in both detectors. Two end-cap calorimeters, alternating steel and proportional chambers, provide calorimetry at angles greater than  $10^\circ$  from the beam. The solid angle subtended by calorimeters is therefore about 98% of  $4\pi$ . Both the hadron calorimeter and the end caps are surrounded by toroid coils, which provide a field of 17 kG.

The entire calorimetric detector is surrounded by drift chambers whose purpose is muon tracking. These chambers determine the radial and axial components of the location and direction of particles penetrating the hadron calorimeters. For the present analysis, chambers covering all of the central hadron calorimeter and much of the end caps are used, subtending a total solid angle of 77% of  $4\pi$ . Five of the sextants have four layers of cylindrical drift cells, each with 88 cells per sextant, while the remaining sextant has three layers of drift planes.

The parent sample for this analysis consists of 25 000 multihadron events, selected according to the following criteria, based on either tracking information or energy flow vectors constructed from calorimeter information: An event must have (1) more than four charged prongs, (2) total visible energy in all calorimeters greater than the beam energy, (3) a scalar sum of the component of the energy vectors perpendicular to the beam greater than 9 GeV, and (4) a vector sum of the energy vectors with magnitude less than 55% of the visible energy. The sample corresponds to integrated luminosities of  $52 \text{ pb}^{-1}$  at 29 GeV center-of-mass energy and  $2 \text{ pb}^{-1}$  at 28 GeV. Within these events, tracks reconstructed

in the drift chambers surrounding the calorimeter constitute muon candidates. A momentum assignment is made for each of these tracks by extrapolating it back through the toroidal magnetic field of the calorimeter to the primary event vertex, taking into account the ionization loss of the particle in the calorimeter. In order to obtain the azimuthal component of the momentum vector, it is required that the track be matched to a segment reconstructed from the energy deposited in the central or end-cap calorimeter. The segment that penetrates to the outermost calorimeter layer and has best agreement in polar angle is the one matched. The momentum resolution is about 30%, due mostly to multiple scattering.

It is required that the momentum assigned to the muon candidate be greater than 2 GeV/c. This cut discriminates against backgrounds both from the decay in flight of pions and kaons to muons, which is more copious for particles with low momenta, and from leakage of particles from hadronic cascades in the calorimeters ("punch-through"). The latter particles often emerge at wide angles with respect to the incident hadron direction, leading to a soft apparent momentum spectrum. Further discrimination against punch-through is achieved by rejecting candidate tracks (1) with path length through the iron in the calorimeters less than about 80 cm (one-third of the candidates are removed by this cut); (2) with evidence in the outer drift chamber of more than one particle having emerged from the calorimeter in the same vicinity (17% of candidates removed); or (3) with ionization in the outermost calorimeter layer in more than two adjacent segments (5% of candidates removed). A few nonhadronic events are removed from the remaining sample by scanning. The final sample contains 476 events.

To estimate the remaining background and to study heavy flavor decay, we have constructed a Monte Carlo model to simulate the production and decay of hadrons<sup>5</sup> and to trace in detail their interactions and the response of the detector.<sup>6</sup> With this model, we find the level of background remaining in the sample from  $\pi$  and  $K$  decays to be  $(23 \pm 1)\%$ . The calculation also provides the spectra for both decay and punchthrough backgrounds used in the analysis described below.

Because the magnitude of the punchthrough background is sensitive to the modeling of the tails of distributions, we determine this level empirically. The hadronic decays of tau leptons provide a source of purely hadronic jets. From a sample of 1600 tau pair events, we find roughly three

muon candidates in hadronic jets attributable to punchthrough, after the decay contribution has been subtracted. Differences between the energy spectra of tau and multihadron jets are accounted for by taking the ratio of the energy deposited in the outermost calorimeter layer in the two samples. From these studies, we find the punchthrough fraction in the inclusive muon sample to be  $(9 \pm 7)\%$ . The probability for the overlap of punchthrough with a genuine muon is small enough that any bias introduced in the cuts designed to reduce the background is negligible.

The fragmentation function of a quark is defined as the probability distribution of the fragmentation variable  $z$ , which is the fraction of a quark's  $E+p_{\parallel}$  ( $p_{\parallel}$  denotes the component of momentum along the original quark axis) carried off by the meson containing that quark. According to the model of Field and Feynman,<sup>7</sup> one of a pair of quarks from the sea is the other constituent of that meson, and the remaining  $E+p_{\parallel}$  is taken by the other member of the pair, which fragments by drawing further pairs of quarks from the sea. The fragmentation functions for the light quarks are well understood, and peak at low values of  $z$ . Theoretical arguments<sup>8</sup> favor a function that is peaked at higher values of  $z$  for greater quark mass.

Since it is the meson containing the heavy quark that decays, producing a muon, the momentum spectrum of the mesons will determine that of the muons. But for each quark flavor, the distribution of the component of the muon's momentum perpendicular to the thrust axis ( $p_{\perp}$ ) is roughly independent of the fragmentation function, except for normalization. Shown in Fig. 1 is the  $p_{\perp}$  spectrum of the observed muons, along with Monte Carlo predictions for muons from  $b$  and  $c$  quarks and the overall (decay plus punchthrough) back-

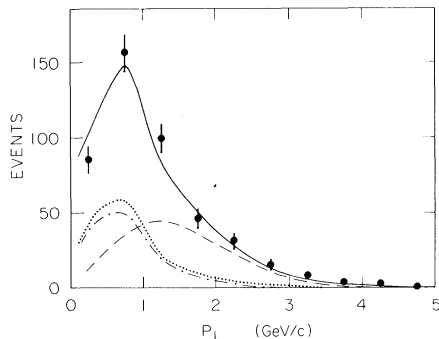


FIG. 1.  $p_{\perp}$  spectrum of muons with  $b\bar{b}$  (dashed curve),  $c\bar{c}$  (dot-dashed curve), background from decay and punchthrough (dotted curve), and total (solid curve) predictions.

ground prediction. The  $b$ - and  $c$ -quark predictions are normalized according to the best fit obtained as described below. It should be noted that the background is concentrated at low values of  $p_{\perp}$ , and is well separated from the  $b\bar{b}$  predicted spectrum. For this reason, the  $b$ -quark fragmentation results presented below are insensitive to the exact level of background that is present, and therefore are not highly dependent on the choice of cuts described above.

As we have noted, the muon's total momentum is sensitive to the fragmentation function, while cuts on  $p_{\perp}$  are useful in obtaining samples enriched in  $c\bar{c}$  or  $b\bar{b}$  events. Accordingly, events were binned by  $p$  and  $p_{\perp}$  into a twenty-element array with  $p_{\perp}$  lower limits at 0, 0.5, 1, and 1.5 GeV/c, and  $p$  lower limits at 2, 3, 4, 5, and 6 GeV/c. In order to use these data to constrain the fragmentation functions, the functions for the  $c$  and  $b$  quarks were approximated by coarse (six-interval) histograms with adjustable heights for each  $z$  interval. Monte Carlo events were generated with use of these "functions," and the heights of the  $z$  intervals and the overall  $c$ - and  $b$ -quark branching ratios to muons were adjusted to obtain best fits to the data. Fits were constrained so that the histogram for each quark was appropriately normalized, the heights were non-negative, and each resulting histogram approximation of a fragmentation function had a single peak. For the  $c$  quark, the six regions of  $z$  are equal divisions of the range  $0 < z_c < 1$ . For the  $b$  quark, the regions of  $z$  equally divide the range  $0.4 < z_b < 1$ ; all functions compatible with the data have small values for  $0 < z_b < 0.4$ .

Figure 2 shows the momentum spectrum for muons with  $p_{\perp} > 1.5$  GeV/c, the region containing the highest fraction of  $b\bar{b}$  events. The dashed lines illustrate the effect of fixing the  $b$  fragmen-

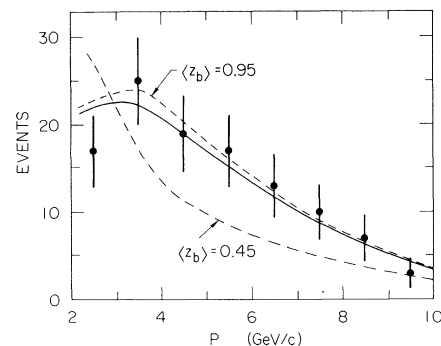


FIG. 2. Total momentum of muons with  $p_{\perp} > 1.5$  GeV/c. Dashed curves are the best fits obtained with the  $b$  fragmentation fixed to a narrow range of  $z$ . The solid curve is the best overall fit.

tation function at particular values of  $z$  (i.e., only one interval of  $z$  has nonzero weight), and allowing the  $c$  fragmentation function and the semileptonic branching fractions of both quarks to vary to obtain best fit to the  $p$  by  $p_{\perp}$  array. It can be seen that low values of  $\langle z_b \rangle$  are ruled out. The solid curve is the predicted spectrum for the best fit, allowing all parameters to vary. Note that the range of observed momenta is large compared to the 30% momentum resolution of the detector; it is found that the results are relatively insensitive to the exact value of the resolution.

The shaded region in Fig. 3 is the one-standard-deviation envelope of all  $b$ -quark fragmentation functions with predicted spectra that yield acceptable fits; in other words, it contains the set of all histograms of the  $b$  fragmentation function that are properly normalized, have a single peak, and are consistent with the data. It is found that  $\langle z_b \rangle = 0.8 \pm 0.1$ . A variety of functions produce chi-square values that are very close to the best-fit value; all of these have most of their contribution in the interval  $0.8 < z_b < 0.9$ . The semimuonic branching ratio for the  $b$  quark, averaged over the neutral and charged  $B$  mesons that decay, is found to be  $(15.5^{+5.4}_{-2.9})\%$ .

A broad range of  $c$  fragmentation functions is permitted by the data, with the  $1\sigma$  envelope allowing  $0.17 < \langle z_c \rangle < 0.67$ . The semimuonic branching fraction is found to be  $(7.6^{+9.7}_{-2.7})\%$ ; the large uncertainty is due to the dependence of the branching fraction on the exact fragmentation function.

A specific functional form for fragmentation, suggested by Peterson *et al.*,<sup>9</sup> has

$$D_q(z) \propto \{z[1 - z^{-1} - \epsilon_q/(1 - z)]^2\}^{-1}.$$

For this particular functional form, we find that  $\epsilon_b = 0.008^{+0.037}_{-0.008}$ , but with a somewhat worse chi-square value than for a more sharply peaked function. The function with  $\epsilon_b = 0.008$  is shown in

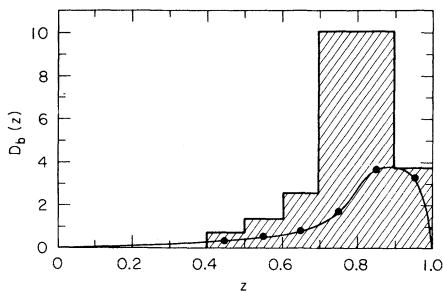


FIG. 3. The shaded region is the envelope of acceptable  $b$ -quark fragmentation functions. The points connected by a curve represent the average value, in each  $z$  interval, of the Peterson *et al.* function (see Ref. 9) for  $\epsilon_b = 0.008$ .

Fig. 3.

In conclusion, the fragmentation of the  $b$  quark is determined to be peaked at  $z_b \approx 0.8$ , in agreement with a result<sup>2</sup> from the Mark II experiment using inclusive electrons. The  $c$ -quark fragmentation function peaks with  $z_c < 0.67$ , a result consistent with direct measurements<sup>1</sup> of the momenta of  $D^*$  mesons. The measured overall semimuonic branching fraction for the  $b$  quark of  $(15.5^{+5.4}_{-2.9})\%$  is consistent with the best measurement.<sup>10</sup> The results of this analysis, therefore, fully confirm the postulated hard fragmentation behavior of heavy quarks.

This work was supported in part by the U. S. Department of Energy under Contracts No. DE-AC02-81ER40025, No. DE-AC03-76SF00515, and No. DE-AC02-76ER00881; by the National Science Foundation under Contracts No. NSF-PHY82-15133, No. NSF-PHY79-20020, No. NSF-PHY79-20821, and No. NSF-PHY80-06504; and by the Istituto Nazionale di Fisica Nucleare.

<sup>(a)</sup>Present address: Cyclotron Laboratory, Harvard University, Cambridge, Mass. 02138.

<sup>(b)</sup>Permanent address: CERN, Geneva, Switzerland.

<sup>(c)</sup>Present address: Mechanical Engineering Department, Stanford University, Stanford, Cal. 94305.

<sup>1</sup>H. Abramowicz *et al.*, *Z. Phys. C* **15**, 19 (1982); M. Althoff *et al.*, DESY Report No. DESY 83/10, 1983 (unpublished); W. B. Atwood *et al.*, SLAC Report No. SLAC-PUB-2981, 1982 (unpublished); C. Bebek *et al.*, *Phys. Rev. Lett.* **49**, 610 (1982); N. Ushida *et al.*, *Phys. Lett.* **121B**, 292 (1983); J. M. Yelton *et al.*, *Phys. Rev. Lett.* **49**, 430 (1982).

<sup>2</sup>M. E. Nelson *et al.*, *Phys. Rev. Lett.* **50**, 1542 (1983).

<sup>3</sup>W. T. Ford, in Proceedings of the International Conference on Instrumentation for Colliding Beam Physics, SLAC Report No. SLAC-250, 1982 (unpublished). See also G. Gidal, B. Armstrong, and A. Rittenberg, Lawrence Berkeley Laboratory Report No. LBL-91 Suppl., 1983 (unpublished).

<sup>4</sup>W. T. Ford *et al.*, *Phys. Rev. Lett.* **49**, 106 (1982).

<sup>5</sup>A. Ali, E. Pietarinen, and J. Willrodt, DESY Report No. DESY T-80/01, 1980 (unpublished).

<sup>6</sup>Electromagnetic showers are simulated by EGS, described by R. L. Ford and W. R. Nelson, SLAC Report No. SLAC-210, 1978 (unpublished). Hadronic cascades are simulated by HETC, described by T. W. Armstrong, in *Computer Techniques in Radiation Transport and Dosimetry*, edited by W. R. Nelson and T. M. Jenkins (Plenum, New York, 1980).

<sup>7</sup>R. D. Field and R. P. Feynman, *Nucl. Phys.* **B136**, 1 (1978).

<sup>8</sup>J. D. Bjorken, *Phys. Rev. D* **17**, 171 (1978); M. Suzuki, *Phys. Lett.* **71B**, 139 (1977).

<sup>9</sup>C. Peterson, D. Schlatter, I. Schmitt, and P. M. Zerwas, *Phys. Rev. D* **27**, 105 (1983).

<sup>10</sup>K. Chadwick *et al.*, *Phys. Rev. D* **27**, 475 (1983).